

# Distribution Function Analysis of Mesoscopic Hopping Conductance Fluctuations

R. J. F. Hughes<sup>†§</sup>, A. K. Savchenko<sup>‡</sup>, J. E. F. Frost<sup>†</sup>, E. H. Linfield<sup>†</sup>, J. T. Nicholls<sup>†</sup>,  
M. Pepper<sup>†</sup>, E. Kogan<sup>§</sup> and M. Kaveh<sup>§</sup>

<sup>†</sup> *Cavendish Laboratory, Madingley Road, Cambridge CB3 0HE, U.K.*

<sup>§</sup> *Minerva Center, Jack and Pearl Resnick Institute of Advanced Technology, Dept. of Physics,  
Bar-Ilan University, Ramat-Gan 52900, Israel.*

<sup>‡</sup> *Department of Physics, University of Exeter, Stocker Road, Exeter EX4 4QL, U.K.*

(October 20, 2018)

## Abstract

Variable-range hopping (VRH) conductance fluctuations in the gate-voltage characteristics of mesoscopic GaAs and Si transistors are analyzed by means of their full distribution functions (DFs). The forms of the DF predicted by the theory of Raikh and Ruzin have been verified under controlled conditions for both the long, narrow wire and the short, wide channel geometries. The variation of the mean square fluctuation size with temperature in wires fabricated from both materials is found to be described quantitatively by Lee's model of VRH along a 1D chain. Armed with this quantitative validation of the VRH model, the DF method is applied to the problem of magnetoconductance in the insulating regime. Here a non-monotonic variation of the magnetoconductance is observed in Si MOSFETS whose sign at low magnetic fields is dependent on the channel geometry. The origin of this defect is discussed within the framework of the interference model of VRH

magnetoconductance in terms of narrowing of the DF in a magnetic field.

PACS numbers: 72.20.-i,72.20.My,73.40Qv,73.50.Jt

## I. INTRODUCTION

Mesoscopic conductance fluctuations in the insulating regime of small, disordered transistors were first observed by Pepper<sup>1</sup> in GaAs MESFETs and then studied in detail in Si MOSFETs by Fowler, Webb and coworkers<sup>2</sup> in the early 1980s. Extremely strong random fluctuations, spanning several orders of magnitude, were observed at low temperatures in the conductances of narrow-channel devices as the gate voltage was varied. At first the origin of this effect was not clear. Azbel<sup>3</sup> suggested that resonant tunneling from source to drain might produce such structure as the chemical potential was swept through transmission resonances of the eigenstates in the random impurity potential. However, it became clear that this zero-temperature mechanism could not make a significant contribution to the conductance in the relatively long devices of this experiment. Instead, the most satisfactory explanation was provided by Lee<sup>4</sup> who proposed a model in which electrons move by variable-range hopping (VRH) along a one-dimensional (1D) chain. A number of elementary hopping resistances, each depending exponentially on the separation and energy difference between sites, are added in series to give the overall resistance of the chain. In this model it is assumed that, because of the extremely broad distribution of the elementary resistors, the total chain resistance can be well approximated by that of the single most resistive hop. The fluctuations then arise as a consequence of switching between the pairs of localized sites responsible for the critical hop as each elementary resistance reacts differently to a change in the chemical potential. These fluctuations are therefore of “geometrical” origin, arising from the random positioning of localized sites in energy and space, as distinct from the “quantum” nature of the tunneling mechanism which would be strongly affected for example by an applied magnetic field.

Serota, Kalia and Lee<sup>5</sup> went on to simulate the ensemble distribution of the total chain resistance  $R$  and its dependence on the temperature  $T$  and the sample length  $L$ . In their ensemble, the random impurities are distributed uniformly in energy and position along the chain. In experiments a single device is generally used, so that the impurity configuration is

fixed, and fluctuations are observed as a function of some variable external parameter such as the chemical potential. An ergodicity hypothesis is then invoked to the effect that the same ensemble is sampled in both cases, something that has been verified experimentally by Orlov *et al.*<sup>6</sup>. Using the natural logarithm of the resistance, the authors of Ref. 5 obtained for the mean and standard deviation:

$$\langle \ln R \rangle \sim \left( \frac{T_0}{T} \right)^{1/2} \left[ \ln \left( \frac{2L}{\xi} \right) \right]^{1/2} \quad (1)$$

$$s \equiv \langle (\ln R - \langle \ln R \rangle)^2 \rangle \sim \left( \frac{T_0}{T} \right)^{1/2} \left[ \ln \left( \frac{2L}{\xi} \right) \right]^{-1/2} \quad (2)$$

where  $\xi$  is the localization radius and  $T_0$  is the characteristic temperature for Mott VRH:  $T_0 = 1/k_B \rho \xi$  ( $\rho$  is the density of states at the Fermi energy). It can be seen that the size  $s$  of the fluctuations decreases extremely slowly with length, a result characteristic of 1D which was first pointed out by Kurkijarvi<sup>7</sup>. The explanation is simply that exceptionally large resistance elements, even though they may be statistically rare, dominate the overall resistance since they cannot be by-passed in this geometry. The averaging assumed in the derivation of Mott's hopping law for 1D does not occur and the total resistance takes on the activated form of the largest individual element.

A detailed analytical treatment of this model was undertaken by Raikh and Ruzin<sup>8,9</sup> who divided the problem up into a number of length regimes. Their theory introduces the concept of the “optimal break”, the type of gap between localized states (on an energy versus position plot) which is most likely to determine the overall resistance. The optimal shape of such a state-free region has maximal resistance for the smallest area and turns out to be a rhombus. A sufficiently long chain will have many such breaks in series to give a most probable resistance

$$R_{\text{prob}} = R_0 \frac{L}{\xi} \left( \frac{T_0}{T} \right)^{1/2} \exp \left( \frac{T_0}{2T} \right)^{1/2} \quad (3)$$

where  $R_0$  is the prefactor in the Mott VRH formula. This formula breaks down once the expected number of optimal breaks in the chain becomes small, of order one. It is valid only when  $\nu \gg 1$ , where  $\nu$  is a parameter defined implicitly by

$$\nu = \frac{2T_0}{T} \ln \left( \frac{L\nu^{1/2}}{\xi} \right) \quad (4)$$

For  $\nu < 1$ , which corresponds to the normal experimental situation, the resistance of the chain is determined by a few sub-optimal breaks of which the expected number occurring in a chain of length  $L$  is approximately one. The most probable resistance, or its logarithm  $Q$ , then follows a more complicated temperature law of the form:

$$Q \equiv \ln \frac{R}{R_0} = \frac{\nu^{1/2} T_0}{T} \approx \left\{ 2 \frac{T_0}{T} \ln \left[ \frac{L}{\xi} \left( \frac{T_0}{T} \right)^{1/2} \ln^{1/2} \left( \frac{L}{\xi} \right) \right] \right\} \quad (5)$$

The probability distribution function (DF) for the quantity  $f(Q)$  is best written in terms of  $\nu$  and a new parameter  $\Delta$ . For  $\nu < 1$  it is given by the following integral:

$$f(\Delta) = \frac{e^\Delta}{\pi} \int_0^\infty dx \exp \left( -x^{\nu^{1/2}} \cos \frac{\pi \nu^{1/2}}{2} \right) \cos \left( x e^\Delta - x^{\nu^{1/2}} \sin \frac{\pi \nu^{1/2}}{2} \right) \quad (6)$$

$$\Delta \equiv Q - \frac{\nu^{1/2} T_0}{T} \quad (7)$$

$f(\Delta)$  is a function with a peak close to  $\Delta = 0$  and width determined by  $\nu$ . In principle it can be written in terms of  $\xi$  and  $\rho$  using Equations (4) through (7). There is a simple relationship between  $\nu$  and the variance of  $Q$ :

$$\langle Q^2 \rangle - \langle Q \rangle^2 = \frac{\pi^2}{6} \left( \frac{1}{\nu} - 1 \right) \quad (8)$$

This theory is equally applicable<sup>10</sup> to the case of the transverse conductance  $G$  of a thin film or barrier. Instead of a sum of series resistances, the required quantity is the sum of parallel conductances representing conducting chains of hops traversing the film. Whereas in 1D the total resistance is determined by the blocking effect of the critical hop, here the total conductance is dominated by an optimal ‘‘puncture’’: an uncommonly high-conductance hopping chain through the barrier which effectively shorts out all other current paths. On a logarithmic scale, since  $\ln R = -\ln G$ , the DFs for the two geometries are simply reflections of each other. The variation of the width and peak position with  $\xi$  and  $\rho$  is different, however, in the two cases. Fig. 1 shows schematics of the two geometries, the equivalent resistor

networks and DFs from Equation (6) characteristic of each case. Here, as throughout the remainder of the paper, the abscissa is  $\ln G$ . In 1D the importance of blocking resistors adds weight to the contribution of extremely high resistances and produces a long tail out to low values of  $\ln G$ . For a short 2D barrier the DF has the opposite asymmetry with a tail out to high conductances, reflecting the effect of punctures in shorting out less conductive paths. In fact the form of the DF is universal, the theory requiring only that the elementary quantities to be summed are independent and come from an exponentially wide distribution. The microscopic details of the conduction mechanism enter only into the dependence of  $\nu$  and  $\Delta$  on external parameters such as the temperature and magnetic field. The requirement of independence in the case of the barrier means that conductive chains must be sufficiently far apart, which should be satisfied for a barrier with a sufficiently large aspect ratio  $W/L$ . We use the description “short 2D” for this short-, wide-channel geometry to distinguish it from the square 2D geometry in which conduction is via an interconnected percolation network.

While the above theory is that best suited to the hopping regime, numerous authors<sup>11</sup> have examined the problem of the *zero-temperature* conductance distribution of disordered wires and they find that, for a sufficiently long wire, the DF is Normal in  $\ln G$ . Some authors<sup>12</sup> argue that this is also the case for the insulating regime in higher dimensions. To obtain a finite-temperature result, it is necessary to introduce a temperature-dependent coherence length. Kramer *et al.*<sup>13,14</sup> have used the Mott hopping length for this purpose and performed an average over localization lengths to calculate the size of the fluctuations in  $\ln G$ . (The Lee model does not allow for a distribution of localization lengths). With the caveat that it is difficult to rigorously justify the averaging method, they find that the size of the fluctuations varies with temperature in  $d$  dimensions as

$$s \simeq \left(\frac{T_0}{T}\right)^{1/2(d+1)} \quad (9)$$

For the case  $d = 1$ , in which we are mostly interested, this yields  $s \sim T^{-1/4}$ , in contradiction with equation (2) which predicts  $s \sim T^{-1/2}$ . An intermediate model<sup>15</sup> describes

fluctuations that are partly geometrical, partly quantum coherent in nature.

The experimental results presented below are able to distinguish between these two theories, providing good quantitative agreement with the geometrical, 1D hopping chain theory. Section III introduces the results on 1D devices in both silicon and gallium arsenide and analyses the temperature dependence of the conductance and its fluctuations in terms of these theories. Section IV exhibits some experimental DFs which are also well described by the theory, both for the 1D and short 2D geometries with their opposite characteristic asymmetric distributions. It is shown that fits to the full DF are more reliable in studying the fluctuation amplitude than just the standard deviation which is prone to large statistical errors due to the long tails. Finally, Section V examines the effect of an applied magnetic field and suggests interesting possibilities for investigating the complicated area of hopping magnetoconductivity by means of experimental DFs.

## II. DEVICES AND EXPERIMENTAL METHOD

A number of different devices, both Si and GaAs and in both the 1D and short 2D geometries, were used for this study. The Si MOSFETs were small-area CMOS devices with an oxide thickness of 210Å and self-aligned ohmic contacts. The 2DEG is formed by inversion in the very lightly-doped p-type Si adjacent to the oxide barrier. Lithographic dimensions for the 1D devices ranged from 0.5 to 2 $\mu$ m wide by 5 to 20 $\mu$ m long for the 1D wires and 100 $\mu$ m wide by 1 to 2 $\mu$ m long for the short 2D geometry. Here the designation of length  $L$  always refers to the distance between source and drain. The electronically active dimensions of the channel were estimated from measurements of samples of varying size to be about 0.5 $\mu$ m smaller than these nominal values.

The GaAs devices were fabricated from a simple delta-doped layer of Si donors with a Hall carrier concentration of  $4 \times 10^{11}$  cm $^{-2}$ . Channels were defined by the application of a negative bias to patterned surface gates. The split gate method<sup>16</sup> was used to define 1D wires, while narrow strip gates were used to create short 2D barriers. Beyond the channel definition

voltage, increasing the bias serves to shift the chemical potential in the active region of the device without greatly changing the channel dimensions. Because of the spreading out of the electric field between the edges of the patterned gate and the delta-layer situated  $0.3\mu\text{m}$  below the surface, the dimensions of the electrically active regions differ significantly from the lithographic dimensions. For example, a split gate with gap dimensions 1mm square produces a narrow channel approximately  $0.2\mu\text{m}$  wide and  $1.8\mu\text{m}$  long. This estimate is based on the observation that split gate devices narrower than 0.8mm did not conduct. Strip gates  $30\mu\text{m}$  wide by  $0.5$  to  $2\mu\text{m}$  long were used to produce short 2D barriers in the region of  $0.8\mu\text{m}$  longer than the lithographic thickness. Aside from the ill-defined channel dimensions, a further problem with these devices was the high series resistance resulting from the partially depleted 2DEG region near the gates. For the short 2D devices it was estimated that this series resistance, which varies with gate voltage, would be sufficient to truncate some of the high-conductance fluctuations. Our measurements were taken after brief illumination with light from a red LED, using the persistent photoconductivity effect to reduce the series resistance from the sample leads.

Two-terminal a.c. resistance measurements were taken in dilution refrigerators down to temperatures of  $50\text{mK}$ . For the Si devices, a low-frequency (8-18Hz) excitation voltage of 5 or  $10\mu\text{V}$  was used, depending on the temperature, and saturation of temperature-dependent quantities was observed below about  $70\text{mK}$ . The temperature dependence of, for example, the average conductance flattens out quite abruptly below this temperature. Measurements have been carried out using several different experimental set-ups and it is our experience that the saturation temperature increases monotonically with the observed noise level. For the GaAs devices it was necessary to use a higher excitation voltage to obtain a sufficiently good signal-to-noise ratio and saturation of the average conductance and the fluctuation amplitude was evident below  $200\text{mK}$ . Because of this and the above-mentioned problems most of the data presented here are from Si MOSFETs. However, all of the results in sections III and IV for Si have been reproduced in the GaAs devices, with the same quantitative agreement but somewhat greater uncertainties.

### III. TEMPERATURE DEPENDENCE OF THE MEAN CONDUCTANCE AND FLUCTUATION AMPLITUDE

The first part of the experiment is to determine the Mott parameter  $T_0$  from an analysis of the temperature dependence of the mean value of the conductance. This is for comparison with the value of  $T_0$  needed to explain the size of the fluctuations. Although we expect VRH to be the conduction mechanism, in our mesoscopic device the averaging implicit in Mott's law is not taking place. We therefore first take the logarithm of the measured conductance and then perform a numerical average of the data-points over a suitable range of gate voltage to obtain the quantity  $\langle \ln G \rangle (= - \langle \ln R \rangle)$ . It is important to reach a suitable compromise between choosing a gate voltage interval sufficiently small that  $T_0$  does not vary significantly over its length yet sufficiently wide to meet the requirements of statistical accuracy. More will be said on this matter in section III on DFs where the choice is much more critical. However, thanks to the large number of fluctuations observed at low temperatures, these requirements are easily met.

Experimental data for a long, narrow 19.4 by  $0.6\mu\text{m}$  Si MOSFET channel are presented in Fig. 2, where a section of the gate voltage characteristic has been split into seven intervals for averaging. It is not possible to distinguish between activation laws with inverse temperature exponents of  $1/3$ ,  $1/2$  or even  $1$  from the temperature range we have available. However, there does appear to be a change of gradient in the vicinity of  $0.3\text{K}$ . This could be indicative of a change from 1D to 2D Mott hopping as the temperature is raised and the hopping distance becomes shorter than the sample width. Indeed, if the values of  $T_0$  above  $0.3\text{K}$  are extracted using the 2D formula with exponent  $1/3$ , and values below  $0.3\text{K}$  using the 1D formula with exponent  $1/2$ , equating the hopping lengths in the two formulae yields a crossover temperature of order  $0.5\text{K}$ , roughly consistent with the observed crossover point. If we introduce the known sample width  $W$ , this interpretation allows  $\xi$  and  $\rho$  to be obtained independently. These work out at  $\xi \sim 0.1\mu\text{m}$  and  $\rho \sim 0.3$  times the density of states for a 2D subband in silicon. Both these values are physically reasonable and consistent with

the conduction mechanism being VRH and 1D in nature below 0.3K. We therefore make this assumption and restrict ourselves to the sub-0.3K range in our subsequent DF analysis. Note that the large value of  $\xi$  shows that we are not very deep in the insulating regime.

The next task is to analyze the temperature dependence of the fluctuation amplitude. We take the same gate voltage intervals as before and this time calculate the standard deviation  $s$  of  $\ln G$ . Here a log-log plot of  $s$  against  $T$  does not yield a straight line (hollow circles, Fig. 5(c)). The slope varies from approximately  $-0.5$  to  $-1.5$  depending on the temperature. This upper power is much greater than can be accounted for by any of the theories. However, the standard deviation as calculated directly from the data points is dominated by the contribution from the low-conductance tail of the distribution, where noise and statistical uncertainty is greatest. As a result, we postpone further comment until the next section where a full distribution function analysis can resolve the issue. The problem is not so apparent in a gallium arsenide split-gate device estimated as being  $0.2\mu\text{m}$  wide by  $1.8\mu\text{m}$  long. Here the data points (of which there are only five ranging from 0.2 to 0.5K) best fit the law  $s \sim 0.4T^{-0.6\pm0.1}$ . This supports the model of Lee and of Raikh and Ruzin expressed in equation (2) at the expense of the scaling approach in equation (9) which would predict a power of  $-1/4$ . Moreover, estimating  $\xi \sim 0.1\mu\text{m}$  from the measured value of  $T_0 = 1.6\text{K}$  and the assumption that the value of  $\rho$  is roughly the 2D subband density of states multiplied by the channel width, gives the length-dependent prefactor in equation (2) as  $[\ln(2L/\xi)]^{-1/2} = 0.5$ , very close to the observed prefactor of 0.4. The exact numerical coefficient in Equation (2) is not given by the authors, but our data indicates that it should be close to unity. Thus the limited available gallium arsenide data appears to be perfectly describe by the VRH chain model. For silicon, once the overall shape of the distribution is taken into account, both the power and the numerical coefficient are found to be perfectly in line with the calculations<sup>5,8</sup> based on the 1D VRH model. This will be the conclusion of the following section.

#### IV. EXPERIMENTAL DISTRIBUTION FUNCTIONS: GEOMETRY AND TEMPERATURE DEPENDENCE

An analysis relying solely on the first two moments of the distribution of  $\ln G$  gives only limited information and, where the distribution has long tails as in this case, may give unrepresentative or erroneous results. The aim of this paper is to show that analysis of the full DF from experimental fluctuations in mesoscopic devices can be an important tool for investigating hopping in the mesoscopic regime and may shed light on the processes underlying the macroscopic magneto-conductivity. To start with, we describe our method of obtaining an experimental DF histogram.

The raw data consists of a set of points representing the fluctuations in conductance as a function of some external parameter, usually a gate voltage  $V_g$ . It is important to establish that there is no zero offset error since the first step is to take the logarithm of the conductance. Generating the desired histogram is simply a matter of binning the data points into suitable classes of  $V_g$ , whose width is chosen as a compromise between acceptable resolution and statistical error. The statistical uncertainty is governed not by the total number of data points but by the number of conductance fluctuations in the data-set. If the number of points covering each peak in the characteristic is excessively high, the data may be thinned out before binning by retaining only every  $n$ th point. Care needs to be taken in identifying a “noise floor” in the conductance measurement, below which point the data is meaningless. Such unreliable data cannot be included in the histograms since taking the logarithm magnifies the noise at low conductances and might produce an artificially long tail in  $\ln G$ . Aside from these considerations, the critical decision is in the gate voltage range of the data-set used to generate the histogram. This cannot be made arbitrarily wide since it is the nature of the devices that  $\rho$  and  $\xi$  vary slowly with  $V_g$  as the chemical potential sweeps through the localized states at the edge of the band (whether it be conduction or impurity band in nature). If this variation causes the mean or background conductance level to change significantly over the chosen interval of  $V_g$ , the DF will be smeared out. This

was a problem for Orlov *et al.*<sup>17</sup> who studied the DF of short 2D channels down to 1.2K in GaAs devices similar to our own. To obtain a sufficient number of fluctuations they had to subtract a smooth background from  $\ln G$ , something that cannot be strictly justified and which does not fully solve the problem. Our gate voltage characteristics, measured at much lower temperatures, have the advantage of much denser fluctuations and it is possible to obtain histograms of a satisfactory quality without any background subtraction. As a rough indication, a  $V_g$  range covering 15 or more peaks yields a good histogram provided that the background conductance does not vary by more than about 10-20% of the total distribution width.

An example of DFs calculated from the experimental gate-voltage characteristic of a  $0.2\mu\text{m}$  wide by  $1.8\mu\text{m}$  long GaAs device is reproduced in Fig. 3 from Ref. 18. The characteristic has been split into five intervals so that the variation of the DF as the channel is pinched off can be seen. The decreasing conductance and increasing relative size of the fluctuations translates simply into a distribution which shifts to lower  $\ln G$  and broadens so that it is fit by a theoretical DF from equation (6) with a smaller value of  $\nu$ . The peak position shifts quite markedly between adjacent intervals, suggesting that the choice of interval size is close to its maximum reasonable limit. Unusually, this data shows a non-monotonic variation of the peak position with gate voltage. The effect is specific to this device and its cause is unclear. A final important point is that the experimental limitations on the smallest conductances which can be measured above the noise level severely restricts the usable gate voltage range. Thus a significant portion of the last DF in the figure is already lost in the noise. At the other end of the range, the conductance does not have to get very high before the fluctuations weaken and the assumption of an exponentially broad distribution breaks down: it is for this reason that the first DF does not have a significant 1D tail. Characteristics for DF analysis therefore have to lie within this gate voltage window, implying that it is only possible to study a narrow range of values of the parameter  $T_0$ .

To fit the experimental DFs to equation (6), the integral is calculated on a mainframe computer for all values of  $\nu$  with a resolution of 0.01. These results are stored and used

to perform a two-parameter least-squares fit to the experimental histogram by shifting the computed curve along the  $\ln G$  axis until the optimum fit to the peak position  $\Delta_0$  (which is more precisely the difference between  $\Delta$  and  $\ln G$ ) is found. This is repeated for each value of  $n$  to find the best global least squares fit to  $\nu$  and  $\Delta_0$ .

The results confirm the Raikh and Ruzin theory for the form of the DF under controlled 1D conditions. Other authors have previously examined the DF in the short 2D geometry, notably Orlov *et al.*<sup>17</sup> in n-type GaAs and Popovich *et al.*<sup>19</sup> who claim to have observed a weak asymmetry in a large-area, wide Si MOSFET. Yakimov *et al.*<sup>20</sup> observed a crossover from the 1D to short 2D forms for conduction across thin a-Si films. The thinnest films apparently showed 1D behavior, which is surprising given that here the 2D DF theory should be most applicable. Interestingly, these authors obtain their histograms without relying on the ergodicity hypothesis by measuring a large number of macroscopically identical devices. In this paper we find quantitatively good fits to both distributions under controlled conditions using differently shaped devices on the same chip.

Figure 4 shows three histograms obtained from three MOSFETs fabricated on the same chip. The middle graph shows a reasonable 1D DF, though the situation is not ideal owing to the rather large channel width and almost metallic conductances. The topmost graph shows good agreement between the short 2D theory and experimental data from a device  $2\mu\text{m}$  long by  $100\mu\text{m}$  wide. However, good agreement for this short 2D case is not as ubiquitous in our data as it is for the 1D wires. Frequently the DFs show no clear asymmetric tail at high conductances and are well represented by a Gaussian curve, as in the lower graph. The reasons for this have not been resolved but some observations may provide hints as to possible explanations. The simplest explanation would be to claim that the devices possessed macroscopic inhomogeneities which produced fixed high-current paths and therefore destroyed the desired wide-channeled geometry. However, it is not true that some devices produce good 2D DFs and others are somehow imperfect; it is rather that the 2D asymmetric distribution is only seen in certain regimes. In particular, the asymmetric distribution is observed only, in the most insulating measurable gate voltage range when the distribution

is very wide. The narrow distributions occurring in the more weakly insulating part of the characteristic are invariably symmetric although the converse is not true: sometimes the most resistive part of the characteristic still yields symmetric distributions. Inexplicably, a strong magnetic field of the order of 5-10T helps to restore the asymmetric distribution in these cases. This has been observed in both silicon and GaAs devices. It is perhaps possible that there are other mechanisms at work in the tail of the distribution where the conductance is generally rather high to be truly in the VRH regime. Some such mechanism - perhaps related to resonant tunneling or the increased importance of electron correlations at these higher currents - could be responsible for truncating the high conductance tail in many of our measurements. This question is still unresolved, although we can be certain that the effect is not due to the addition of any series contact resistance since subtracting even the largest plausible values for such a resistance before calculating  $\ln G$  has little effect on the shape of the distributions.

In order to reach the final result of this section, we re-examine the temperature dependence of the fluctuation size using a distribution function analysis rather than simply calculating the standard deviation  $s$  of the data points. Comparison between the two methods shows that DF fits obtained by calculating  $s$  and then using Equation (8) to select the appropriate value of  $\nu$  gives very poor results. This method appears to give good fits to the tail of the distribution, where the experimental histograms are prone to large statistical errors, at the expense of the bulk of the distribution. Reanalysis of the  $19.4\mu\text{m}$  long Si MOSFET shows that the discrepancy between the two methods, while small for the mean log conductance, can be as much as a factor of two in the standard deviation. Fig. 5(a) shows the full set of DFs and their fits to the 1D theory. On the accompanying plots 5(b) and (c), hollow circles represent simple calculations of the mean and standard deviation directly from the data points while full circles are the equivalent quantities calculated from the best fit to the entire DF. Either method results in a similar estimate of the Mott parameter of  $T_0 = 6 - 8\text{K}$  (Fig. 5(b)). For the standard deviation  $s$ , the straightforward method as we saw above gives a  $T^{-1.4}$  power law dependence saturating at low temperatures (in

GaAs at higher temperatures the best power law was  $T^{-0.6}$ ). The full DF analysis, however, yields a straight line on a log-log plot over the entire range with a best fitting power also of  $-0.6$  (Fig. 5(c)). This is very close to the prediction of  $-0.5$  for the 1D chain model and once again disagrees with the result derived from scaling. In Fig. 5(d) the fit to a forced  $-0.5$  power law gives a prefactor of 0.35, very close to the value of 0.4 from the values of  $\rho$  and  $\xi$  estimated in section III. So, in both Si and GaAs devices, Lee's 1D chain hopping chain model gives a quantitatively accurate description of the results, but a reliable analysis requires the distribution function method

## V. VARIATION OF THE DF WITH MAGNETIC FIELD

Having verified the applicability of both the 1D hopping chain theory and Raikh and Ruzin's form of the DF to our devices, it is now possible to use the experimental histograms as a tool with which to investigate the mechanisms of magneto-conductance in the VRH regime. This field has witnessed a large theoretical effort, particularly using the interference mechanism of Nguen, Spivak and Shklovskii<sup>21</sup> (see review<sup>22</sup> and also Refs. 23–26 for more recent calculations). In this model the presence of scatterers between the initial and final sites allows interference to occur between alternative possible paths within a single hop. The phase shifts introduced when a perpendicular magnetic field is applied can give rise to a positive magnetoconductance (PMC) in a macroscopic 2D or 3D sample. The macroscopic conductivity is derived from a logarithmic average over the distribution of elementary hopping conductances, which becomes narrower in a magnetic field. At low fields the peak of this distribution does not shift and the relatively small PMC is a result of the extra weight afforded to low conductances by the logarithmic average<sup>21</sup>. At slightly higher fields it is possible for the peak of the distribution to shift to higher conductances, corresponding to a significant increase in the localization length, and the PMC can be exponentially large<sup>24</sup>.

Experiments<sup>27–30</sup> on 2D gallium arsenide samples widely exhibit PMC in the VRH regime, as does the study on indium oxide films<sup>31</sup>. The interference effects are gener-

ally smaller in silicon devices but PMC has been observed in the 2D inversion layer of MOSFETs<sup>32</sup> and also in narrow-channelled, quasi-1D MOSFET channels<sup>33</sup>. Our devices are not macroscopic so that the precise details of the averaging procedure needed to calculate the magnetoconductance in a 2D percolation network do not concern us. Instead, analysis of the mesoscopic conductance fluctuations in terms of their distribution functions can give direct insight into the elementary distributions at the root of the interference theory, provided that the effect of sample geometry is taken into account. We have already seen that the geometry effect in our samples is well-described by the theory of Raikh and Ruzin. The present section therefore proceeds by introducing some experimental magnetoconductance data, mostly from silicon MOSFET devices, together with a suggestion as to its interpretation in terms of the elementary hopping distribution.

As before, the first approach is to calculate the mean value  $\langle \ln G \rangle$  from a suitable section of the gate voltage characteristic. The variation of  $\langle \ln G \rangle$  with magnetic field  $B$  is obtained from data in which numerous gate voltage sweeps are taken at a series of fixed magnetic fields. Over the full magnetic field range, the gross behavior is similar in GaAs and Si both for 1D and short 2D devices. Fig. 6 shows the variation of  $\langle \ln G \rangle$  with  $B$  in Si MOSFETs of both geometries up to high fields. At temperatures of order 100mK there is a NMC in fields up to about 1T by a factor of order  $e$  followed by a larger PMC up to fields of around 7T. The NMC is not observed in the GaAs devices but the same PMC is evident and is undoubtedly related to the proximity to the insulator-quantum Hall transition also observed in macroscopic devices made from these material<sup>34</sup>. At higher fields, the conductivity rapidly freezes out. These exponentially large changes in conductance are the result of changes in the localization length induced by the magnetic field. At lower fields, of the order of a few tenths of a Tesla, a smaller magnetoconductance is observed in the silicon devices where this field range has been probed in detail. The effect is interesting in that the sign of the magnetoconductance is positive in the case of a 1D wire and negative in the case of a short 2D sample. The presence or absence of such an effect has not been sufficiently investigated in the GaAs devices. Figs. 7 and 8 show the behavior of  $\langle \ln G \rangle$  in the two instances, together

with DFs and samples of the data. In general, the time period necessary to collect all the data for a large number of magnetic fields is too great for the gate voltage sweeps to remain entirely reproducible – this was the case in Fig. 6 and all our experiments to high fields. However, an acceptable degree of reproducibility was achieved for the data presented in the low-field figures. The detailed structure of the characteristic changes substantially over this field range. The overall relative magneto-conductance is in both cases by a factor of order  $e$ . Measurable conductances are only obtainable with hopping lengths of the order  $0.1\mu\text{m}$  so, in this low-field range, the hopping length  $r_M$  and the magnetic length are comparable. With the observed values of  $T_0$  generally around 5K and a measurement temperature of just under 0.1K the hopping length should be several times greater than the localization length so that the condition  $r_M \gg \xi$  demanded by most of the theories is met. For the 1D device, our estimates suggest that  $r_M$  is only slightly greater than the channel width while  $\xi$  is somewhat smaller. We therefore believe that the hopping path is effectively one-dimensional while the channel is wide enough to accomodate the cigar-shaped coherence region of the interference model.

It is not possible to demonstrate conclusively the origin of the different signs observed in the low-field magnetoconductance for these two samples but the following explanation appears the most attractive. According to the interference model, the distribution of elementary hopping conductances narrows on applying a small magnetic field. Our experimental DFs do not directly measure this elementary distribution which is skewed because of the high aspect ratios of our channel geometries. In 1D, because the overall conductance tends to be dominated by difficult hops, the low conductance tail in the elementary distribution is amplified in the experimental DF to produce the characteristic tail out to low conductances. When the elementary distribution narrows slightly under the influence of a magnetic field, the effect on the experimental DF should also be amplified so that the long tail disappears very quickly. Conversely, for the short 2D geometry, the experimental DF is biased in favor of high conductances so that when the elementary distribution narrows, the high conductance tail in our observed DF should rapidly disappear. The result is that a narrowing of the

elementary distribution in a magnetic field, provided that it is not accompanied by a shift in the mean conductance, should result in a positive magnetoconductance for a 1D wire but a negative magnetoconductance for a short 2D channel. This is exactly what we observe in the magnetic field dependence of the average  $\langle \ln G \rangle$  up to about 0.5T. However, a look at the distributions themselves can confirm or disprove this hypothesis.

Taking the 1D case first, the experimental histograms in Fig. 7 immediately show that our hypothesis is reasonable. The low-conductance tail rapidly disappears to the point where the fit to the theoretical 1D DF starts to become dubious. On the other hand, the high-conductance threshold of the distribution does not shift at all, especially when looking at the fitted functions. The overall effect is a shift in the weight of the distribution leading to the PMC shown in the adjacent plot (b). The narrowing of the distribution is apparent in the shrinking of the standard deviation with  $B$  witnessed in Fig. 7(c). Moving next to the 2D case in Fig. 8, we see that the real situation is perhaps more complex. While it is arguable that the high conductance tail starts to disappear at about 0.5T, the low conductance threshold steadily decreases. In fact Fig. 8(c) shows a slight *broadening* of the distribution, completely at odds with the distribution-narrowing hypothesis and with the theoretical calculations. It should be noted that the distributions are somewhat noisy and the fits consequently poorer so that it is difficult to be quantitatively certain of the results. It should also be borne in mind that we do not have a good explanation for the NMC observed at fields of out to 2T in both transistors. Both MOSFETs show this, irrespective of the channel geometry, despite the fact that their construction is not identical.

Evidently then, more questions are raised than are answered. At present the experimental data is very limited and further experiments should help to elucidate the magnetoconductance mechanisms. Given the tantalizingly complicated non-monotonic variation of  $\langle \ln G \rangle$  with  $B$ , further work is clearly desirable. Extension of the measurements to the high-field regime will be difficult because the conductance changes by several orders of magnitude and also because of problems with reproducibility. However, the task could be approached piecewise by analyzing different sections of the gate voltage characteristic for different field

ranges. Detailed examination of the low-field regime in GaAs devices is also a priority.

## VI. CONCLUSION

This paper details an experimental investigation into the use of distribution functions to analyze hopping conductivity in mesoscopic Si and GaAs transistors. A reliable method for obtaining histograms of useful quality has been described and the form of the DF predicted by Raikh and Ruzin for the 1D and short 2D cases verified under controlled conditions. For 1D Si wires, DF analysis is instrumental in showing that the temperature dependence of the fluctuation size is in agreement with the predictions of Lee's model for VRH along a 1D chain. The same quantitative agreement is also found in GaAs wires. Finally, we have shown that experimental distribution functions from mesoscopic devices can provide a useful method of gaining additional insight into the mechanisms of magnetoconductance. In Si MOSFETs at low fields, the dependence of the sign of the magnetoconductance depends on the device geometry, being positive in a narrow quasi-1D device and negative in a short 2D channel. This is what one would expect from a narrowing of the elementary hopping conductance distribution taking into account the selection effects of the channel geometry. For the 1D device, DF analysis shows that the observed PMC in  $\langle \ln G \rangle$  is explicable as a consequence of this narrowing of the elementary distribution as predicted by the interference model. In the slightly more complicated 2D case, this explanation is not supported by the experimental DFs and further experiments are warranted.

The authors are very grateful to G. Citver and V. Ginodman for technical assistance. We would like to thank D. H. Cobden, I. Shlimak and M. E. Raikh for illuminating discussions. RJFH acknowledges support from Trinity College Cambridge and the kind hospitality of Bar-Ilan University. We are grateful to Y. Oowaki for providing a Si MOSFET sample.

## REFERENCES

<sup>1</sup> M. Pepper, J. Phys. C **10**, L173 (1977).

<sup>2</sup> A.B. Fowler, A. Hartstein, and R.A. Webb, Phys. Rev. Lett. **48**, 196 (1982); R.A. Webb, A. B. Fowler, A. Hartstein, and J. J. Wainer, Surface Science **170**, 14 (1986).

<sup>3</sup> M. Ya. Azbel, Solid State Commun. **45**, 527 (1983).

<sup>4</sup> P. A. Lee, Phys. Rev. Lett. **53**, 2042 (1984).

<sup>5</sup> R. A. Serota, R. K. Kalia, and P. A. Lee, Phys. Rev. B **33**, 8441 (1986).

<sup>6</sup> A. O. Orlov, A. K. Savchenko, and A. V. Koslov, Solid State Commun. **72**, 743 (1989).

<sup>7</sup> J. Kurkijarvi, Phys. Rev. B **8**, 922 (1973).

<sup>8</sup> M. E. Raikh and I. M. Ruzin, Sov. Phys. JETP **68**, 642 (1989).

<sup>9</sup> M. E. Raikh and I. M. Ruzin, in *Mesoscopic phenomena in solids*, edited by B. L. Altshuler, P. A. Lee and R. A. Webb (North-Holland, Amsterdam, 1991).

<sup>10</sup> M. E. Raikh and I. M. Ruzin, Sov. Phys. JETP **65**, 1273 (1987).

<sup>11</sup> see e.g. A. A. Abrikosov, Solid State Commun. **37**, 997 (1981).

<sup>12</sup> A. Cohen, Y. Roth, and B. Shapiro, Phys. Rev. B **38**, 12125 (1988).

<sup>13</sup> B. Kramer, A. Kawabata, and M. Schreiber, Phil Mag. B **65**, 595 (1992).

<sup>14</sup> P. Markos and B. Kramer, Ann. Physik **2**, 339 (1993).

<sup>15</sup> F. Ladieu, D. Mailly., and M. Sanquer, J. Phys. I France **3**, 2321 (1993).

<sup>16</sup> T. J. Thornton, M. Pepper, H. Ahmed, and G. J. Davies, Phys. Rev. Lett. **56**, 1198 (1986).

<sup>17</sup> A. O. Orlov, M. E. Raikh, I. M. Ruzin, and A. K. Savchenko, Sov. Phys. JETP **69**, 1229 (1989); Solid State Commun. **72**, 169 (1989).

<sup>18</sup> R. J. F. Hughes, A. K. Savchenko, J. E. F. Frost, M. Pepper, C. J. B. Ford, E. H. Linfield,

M. Grimshaw, D. A. Ritchie, and G. A. C. Jones, in *Hopping and Related Phenomena V* edited by C. J. Adkins, A. R. Long, and J. A. McInnes (World Scientific, 1994), p75.

<sup>19</sup> D. Popovic, A. B. Fowler, S. Washburn, and P. J. Stiles, Phys. Rev. B **42**, 1759 (1990).

<sup>20</sup> A. I. Yakimov, N. P. Stepina, and A. V. Dvurechenskii, Sov. Phys. JETP **75**, 1013 (1992).

<sup>21</sup> V. L. Nguen, B. Z. Spivak, and B. I. Shklovskii, JETP Lett. **41**, 42 (1985); Sov. Phys. JETP **62**, 1021 (1985).

<sup>22</sup> B. I. Shklovskii and B. Z. Spivak, in *Hopping transport in Solids* edited by B. Shklovskii and M. Pollak (Elsevier, 1990), Ch.9.

<sup>23</sup> E. Medina, M. Kardar, Y. Shapir, and X. R. Wang, Phys. Rev. Lett. **64**, 1816 (1990); E. Medina, M. Kardar, Phys Rev B **46**, 9984 (1992).

<sup>24</sup> H. L. Zhao, B. Z. Spivak, M. P. Gelfand, and S. Feng, Phys. Rev. B **44**, 10760 (1991).

<sup>25</sup> W. Schirmacher Phys. Rev. B **41**, 2461 (1990).

<sup>26</sup> M. E. Raikh and G. F. Wessels, Phys. Rev. B **47**, 15609 (1993).

<sup>27</sup> E. I. Laiko, A. O. Orlov, A. K. Savchenko, E. A. Il'ichev, and E. A. Poltoratskii, Sov. Phys. JETP **66**, 1258 (1987).

<sup>28</sup> F. Tremblay, M. Pepper, R. Newbury, D. A. Ritchie, D. C. Peacock, J. E. F. Frost, G. A. C. Jones, and G. Hill, Phys. Rev. B **41**, 8572 (1990).

<sup>29</sup> Q. Ye, B. I. Shklovskii, A. Zrenner, F. Koch, and K. Ploog, Phys. Rev. B **41**, 8477 (1990).

<sup>30</sup> H. W. Jiang, C. E. Johnson, and K. L. Wang, Phys. Rev. B **46**, 12830 (1992).

<sup>31</sup> Z. Ovadyahu, Phys. Rev. B **33**, 6552 (1986).

<sup>32</sup> A. Hartstein, A. B. Fowler, and K. C. Woo, Physica B+C, **117**, 655 (1983).

<sup>33</sup> A. Ohata and A. Toriumi, Surface Science **263**, 157 (1992).

<sup>34</sup> R. J. F. Hughes, J. T Nicholls., J. E. F. Frost, E. H. Linfield, M. Pepper, C. J. B. Ford, D. A. Ritchie, G. A. C. Jones, E. Kogan, and M. Kaveh M., *J. Phys. Condens. Matt.* **6**, 4763 (1994).

## FIGURES

FIG. 1. Device schematics and theoretical DFs for two values of the parameter  $n$ . (a) The 2D device behaves like a sum of parallel conductors and its DF has a tail out to high  $\ln G$ . (b) The 1D device behaves like a sum of series resistances with a tail on the DF towards low  $\ln G$ .

FIG. 2. (a) Part of the experimental characteristic on a logarithmic conductance scale from a  $19.4 \times 0.6\mu\text{m}$  1D Si MOSFET. Dotted lines demarcate gate voltage intervals used for averaging. (b) Fits of this data to the 1D Mott law averaged over the marked gate voltage intervals together with the values of  $T_0$  extracted below 0.3K.

FIG. 3. Conductance fluctuations from a  $1.8 \times 0.2\mu\text{m}$  1D GaAs device and experimental DFs obtained from five adjacent gate voltage intervals spanning the characteristic. At low gate voltages, the distribution is no longer exponentially wide while at high gate voltages the conductance becomes too small to measure. In between is a region where good fits to the theoretical 1D DF (solid curves) can be obtained.

FIG. 4. Distribution functions obtained from three Si MOSFETs fabricated on the same chip showing the characteristic 1D and 2D asymmetries. Lithographic channel dimensions are (length width): (a)  $2 \times 100\mu\text{m}$  fit by 2D DF, (b)  $5 \times 2\mu\text{m}$  fit by 1D DF and (c)  $1.5 \times 100\mu\text{m}$  fit by a Gaussian. Inset are the regions of the characteristic from which the histograms were obtained.

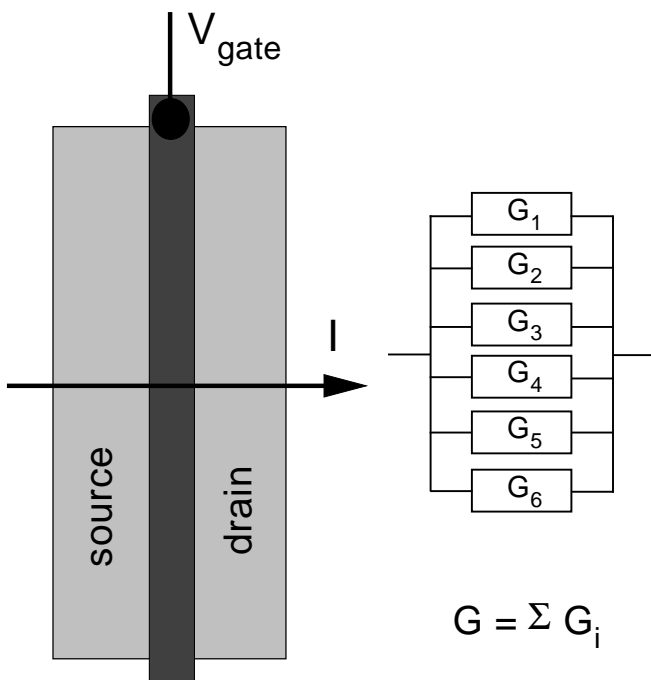
FIG. 5. Temperature dependence of the fluctuations from a  $19.4 \times 0.6\mu\text{m}$  Si MOSFET. (a) Experimental DFs fit by the 1D theoretical form. (b) Fit to Mott's law of the average of  $\ln G$  obtained both directly (hollow circles) and from the position  $\Delta_0$  of the fitted DFs (filled circles). (c) Temperature dependence of the fluctuation amplitude  $s$  both measured by the standard deviation of the data points (hollow circles) and calculated from the fits to the 1D DFs (filled circles). The gradient of the latter yields a  $T^{-0.65}$  power law. (d) Fitting the fluctuation amplitude to a  $T^{-1/2}$  power law yield the prefactor 0.35.

FIG. 6. Average magnetoconductance of Si MOSFETs with the (a) 1D and (b) short 2D geometries. On this scale the low-field PMC is indicated by just the first two points in (a).

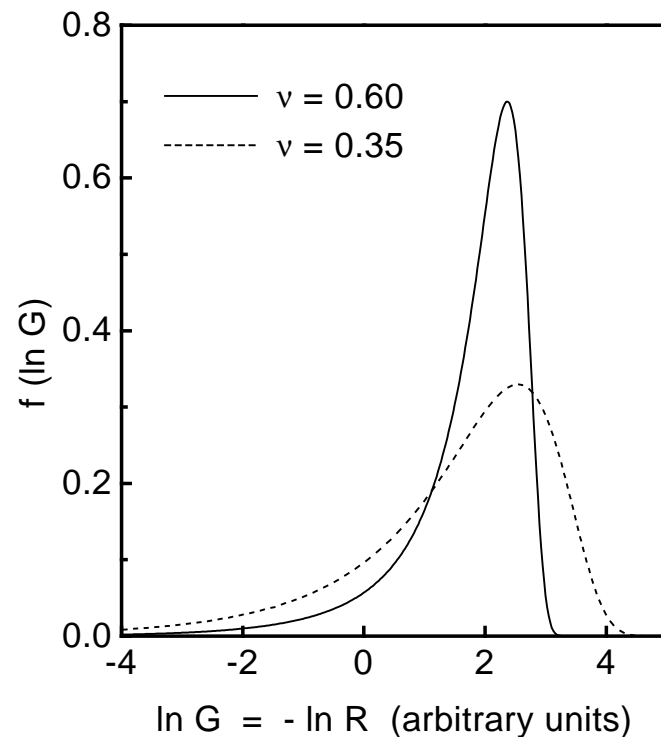
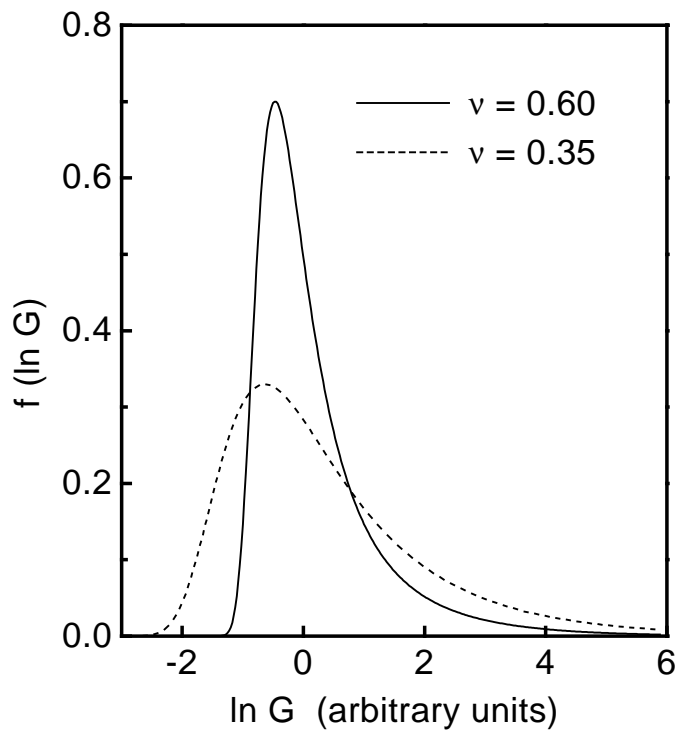
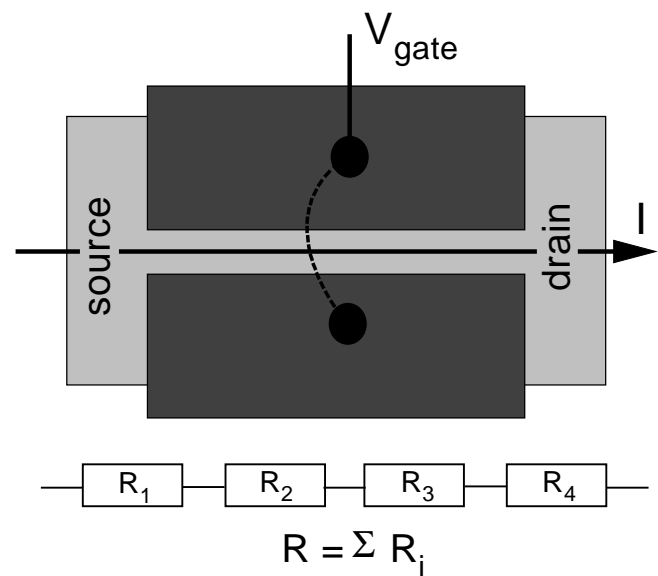
FIG. 7. (a) DFs obtained from a  $19.4 \times 0.6\mu\text{m}$  Si MOSFET as a function of magnetic field and their fits to the 1D theory. (b) The average magnetoconductance obtained by the direct and fitting methods is positive. (c) The standard deviation of the distribution obtained by the two methods decreases.

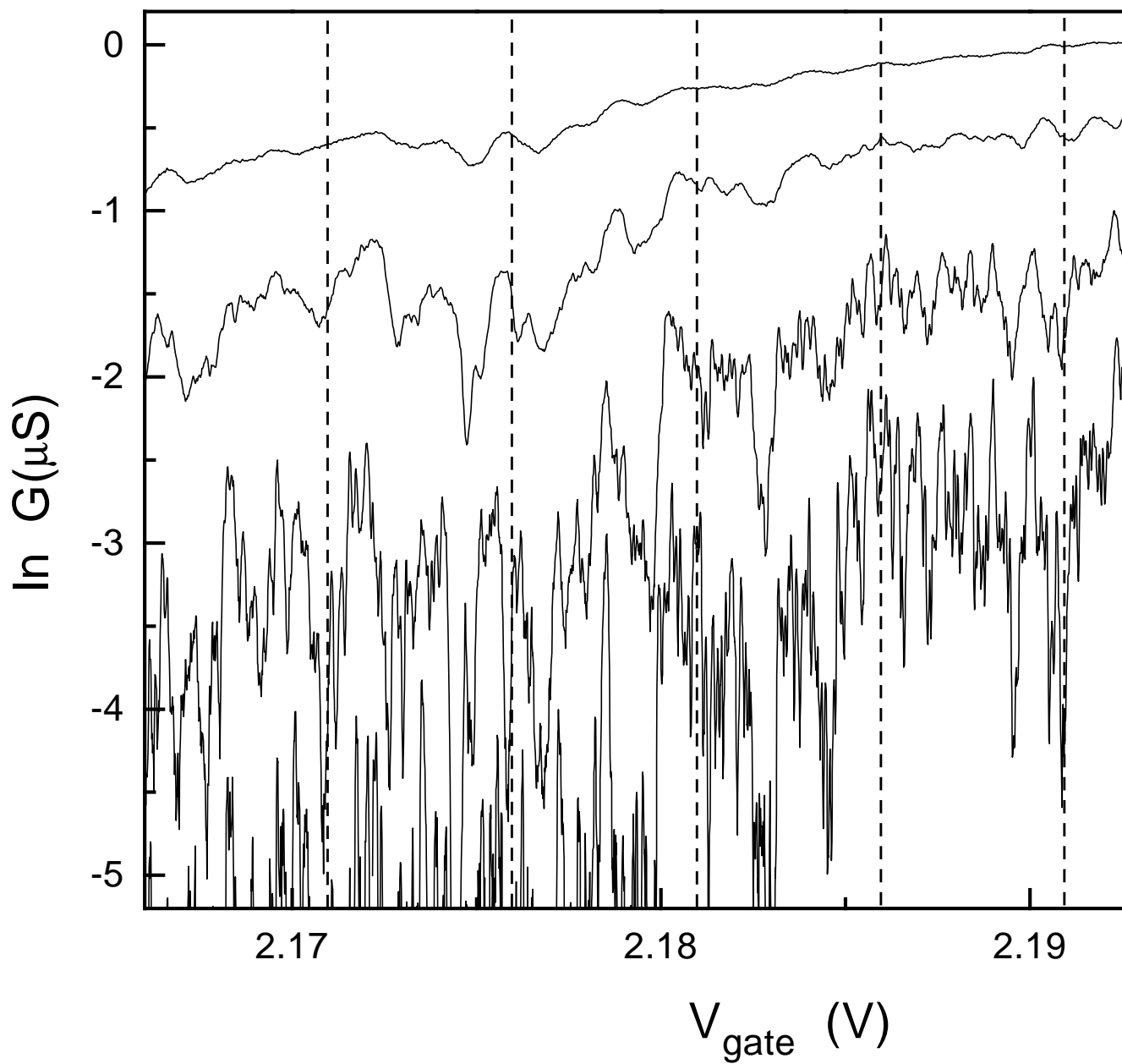
FIG. 8. (a) DFs obtained from a  $2 \times 100\mu\text{m}$  Si MOSFET as a function of magnetic field and their fits to the 2D theory. (b) The average magnetoconductance obtained by the direct and fitting methods is negative. (c) The standard deviation of the distribution obtained by the two methods increases slightly.

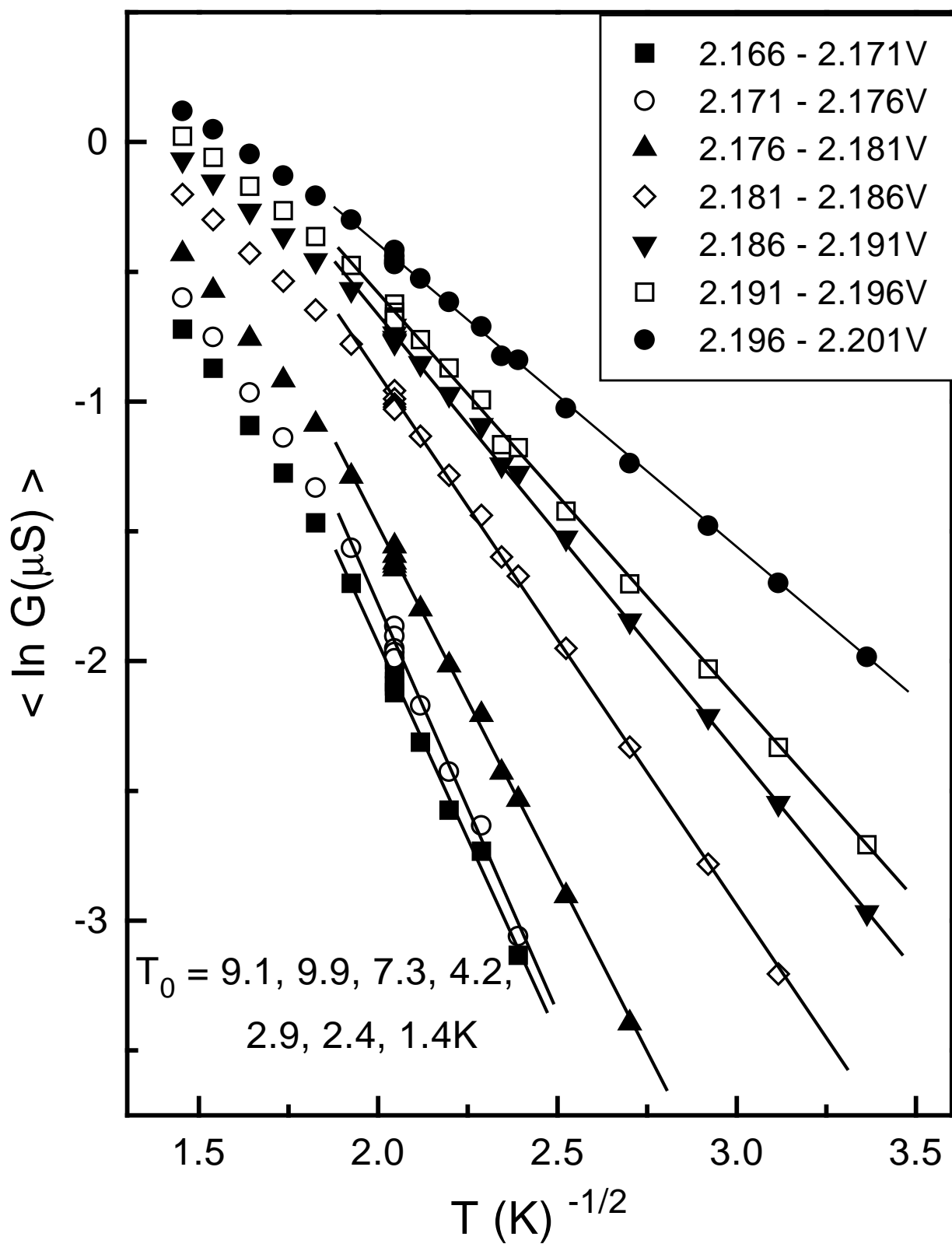
(a)

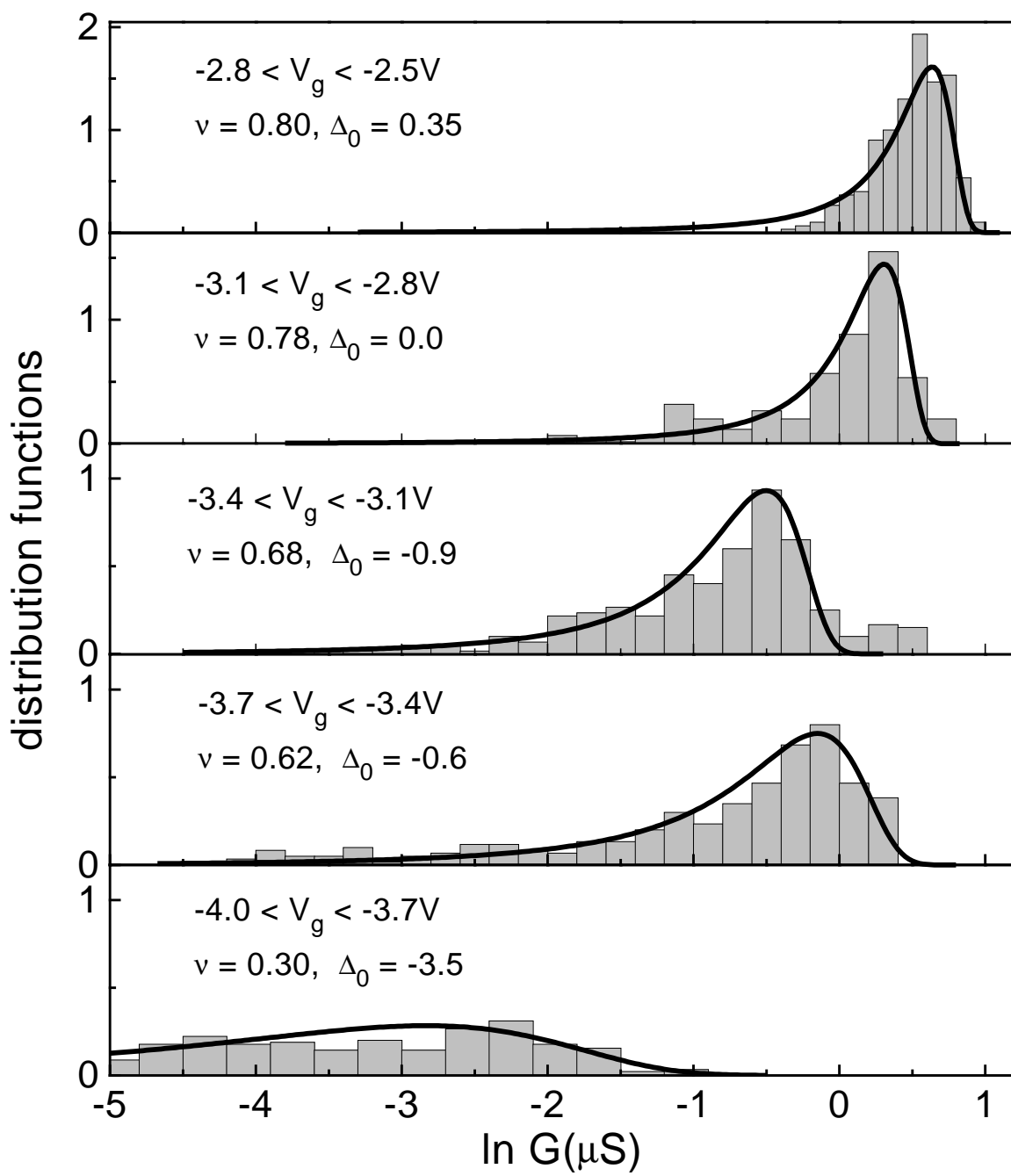
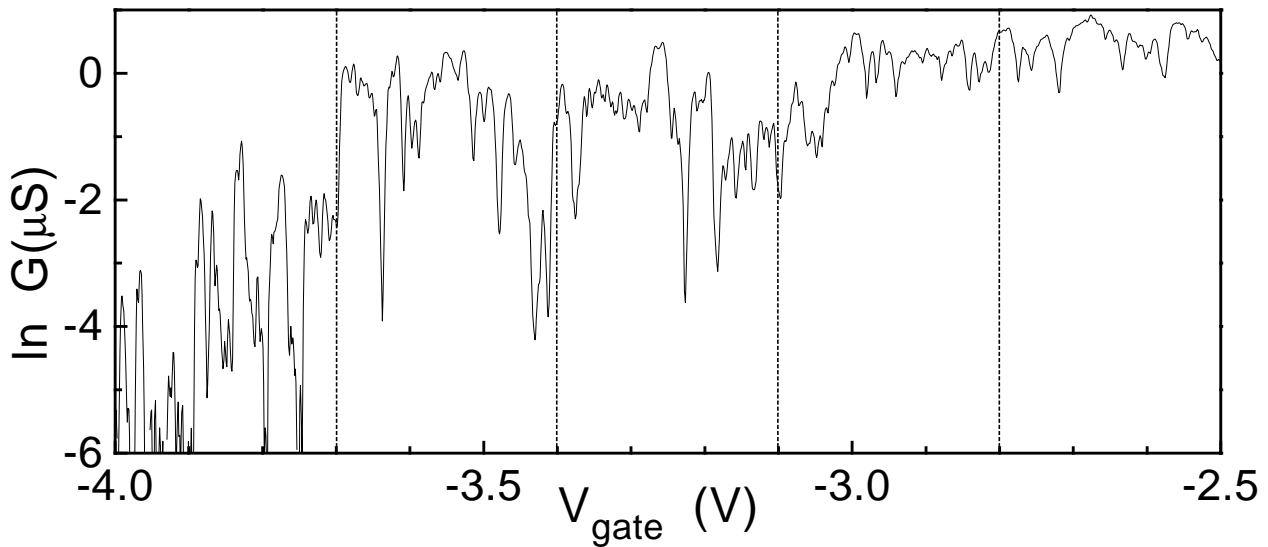


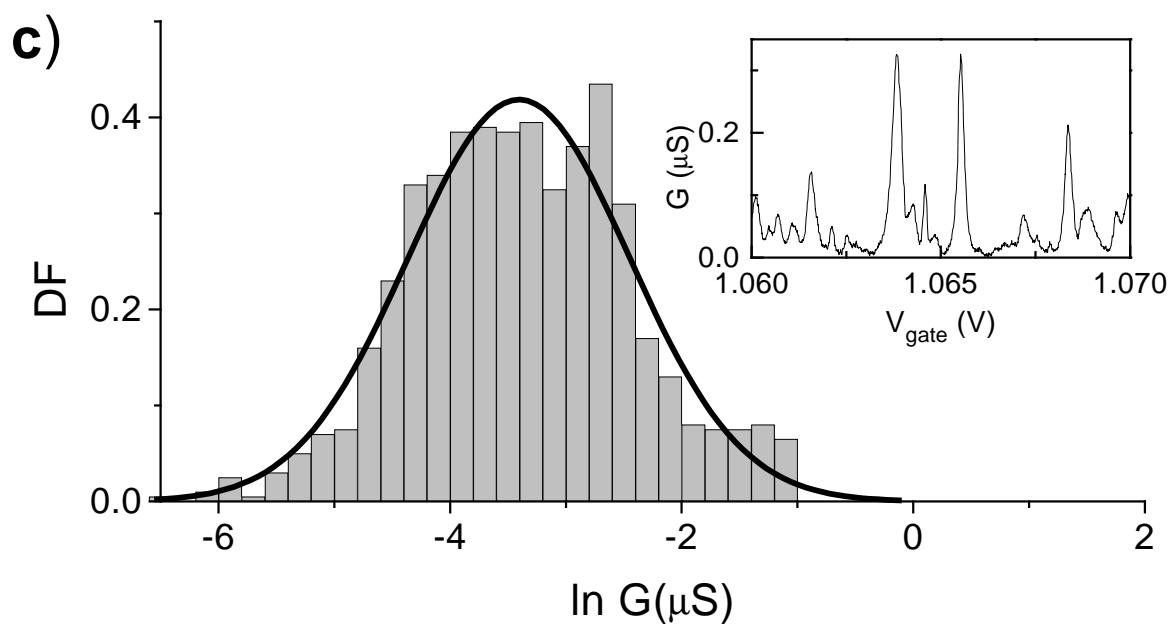
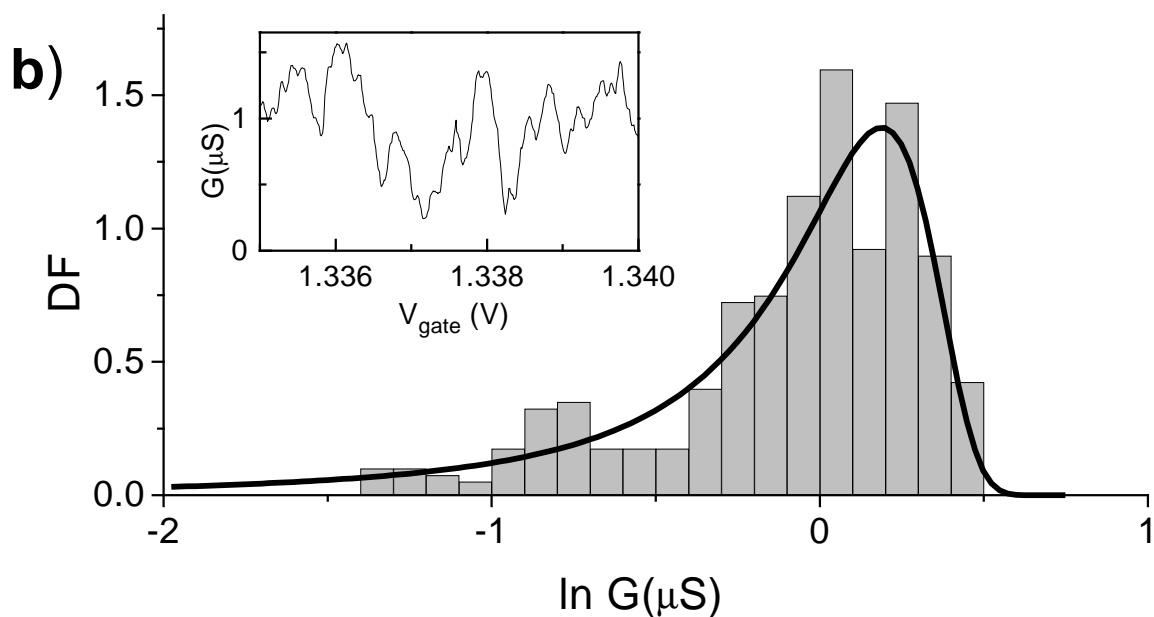
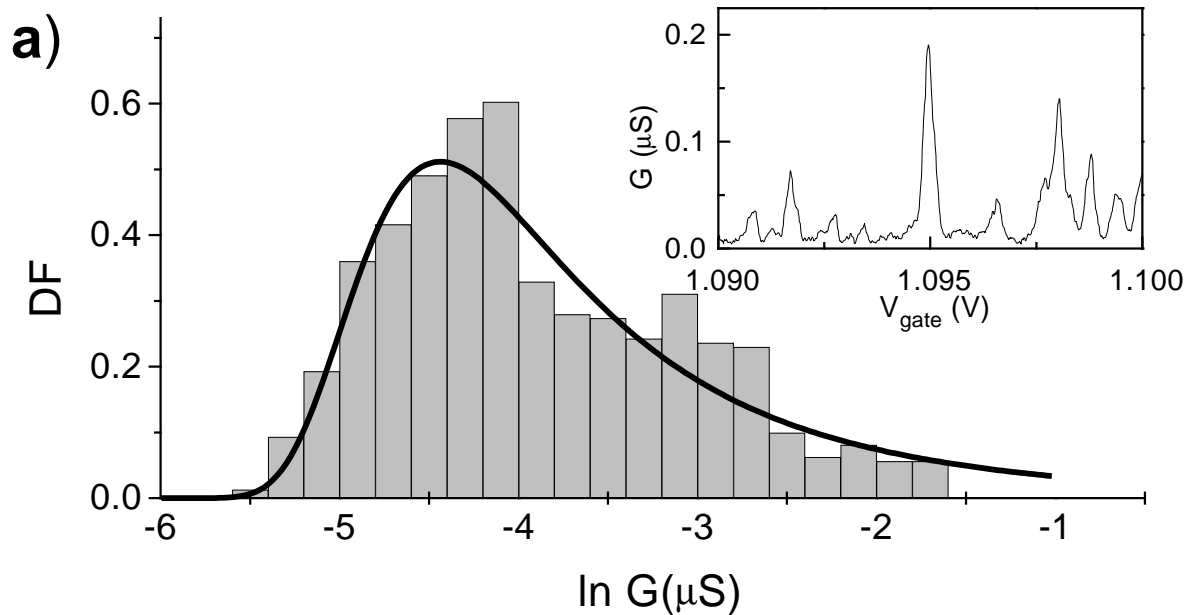
(b)

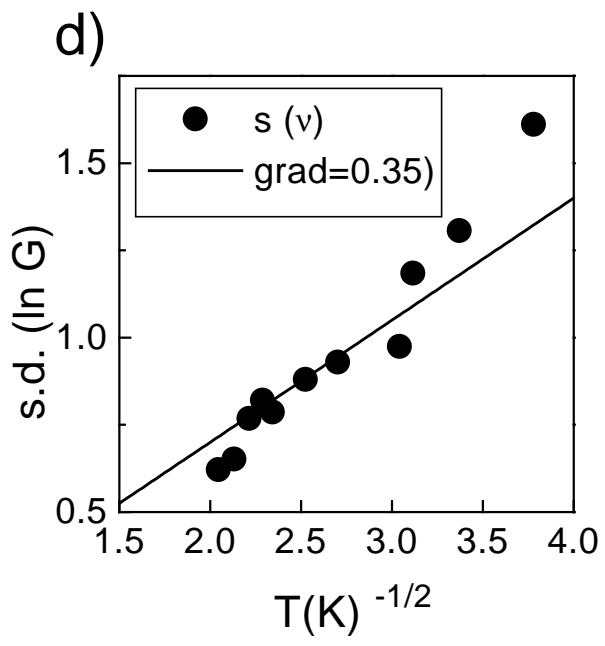
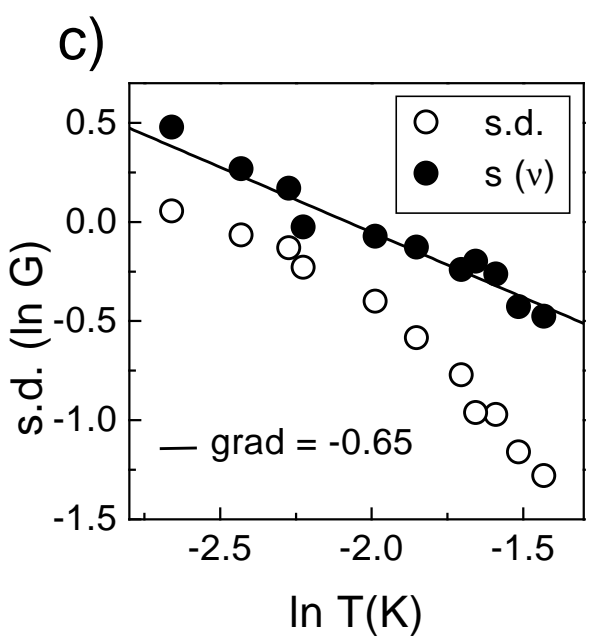
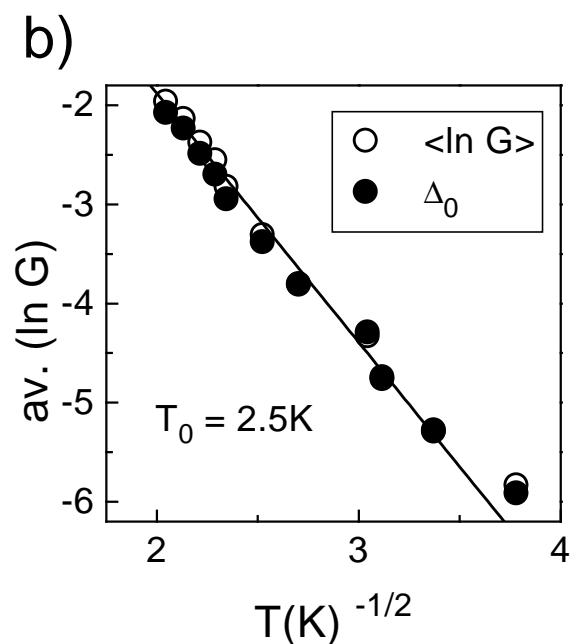
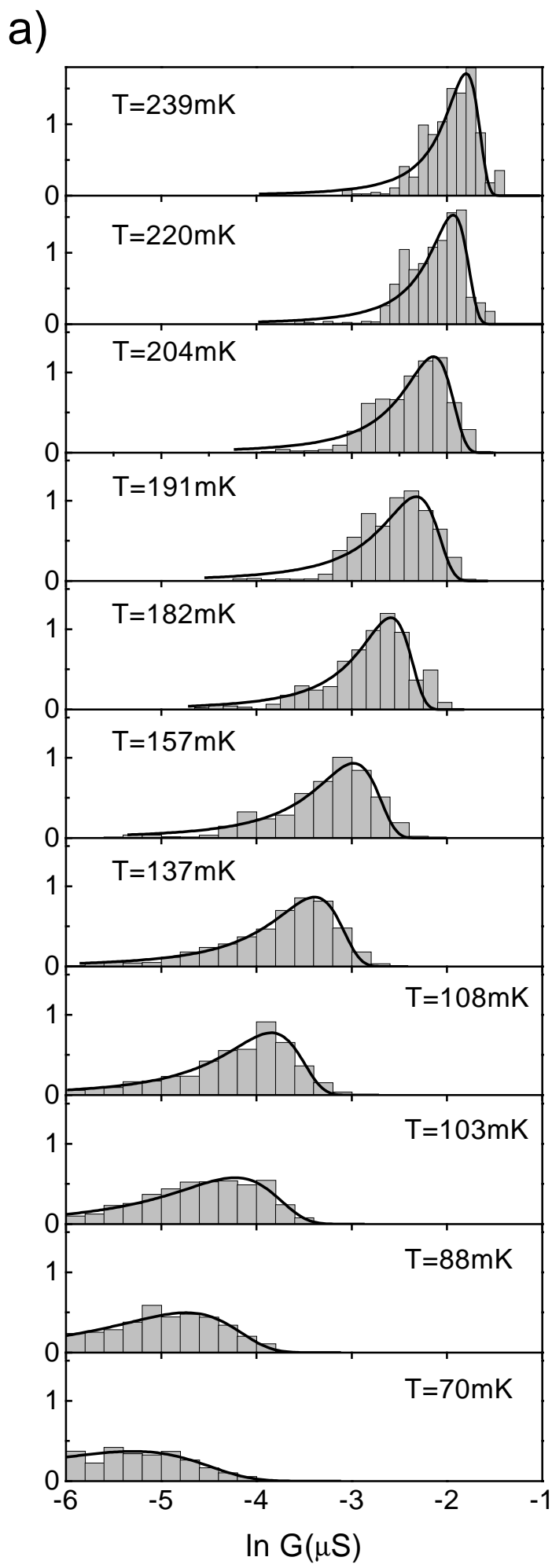


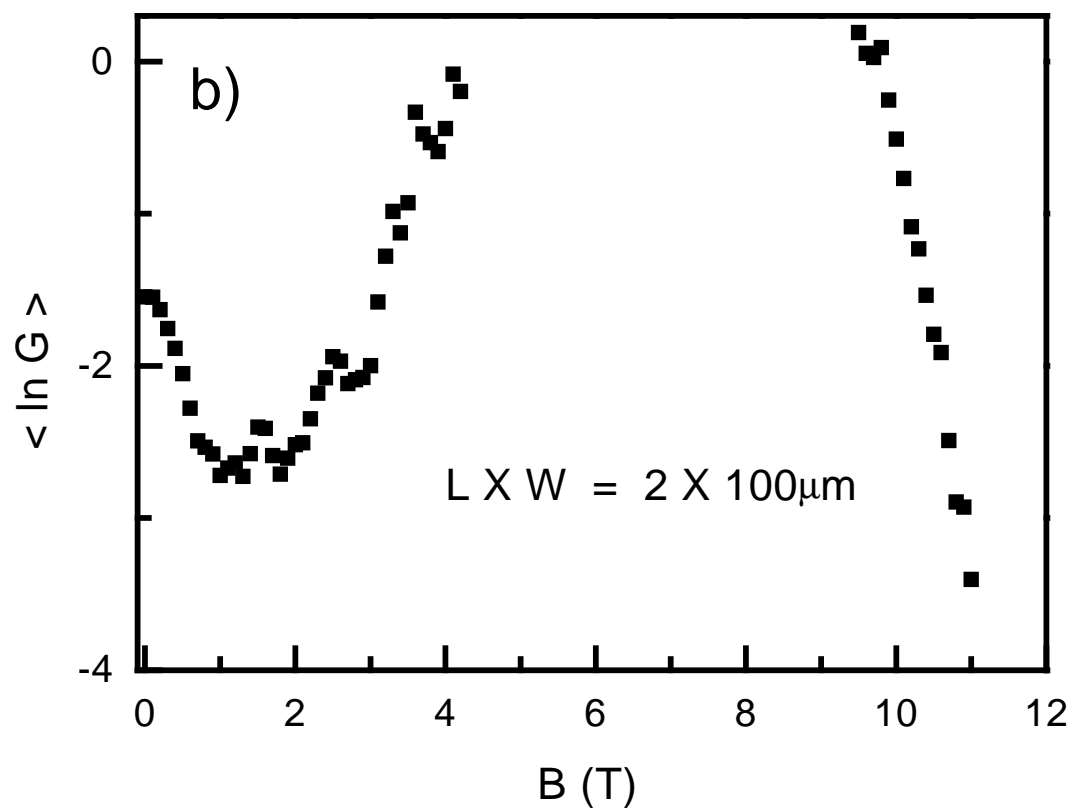
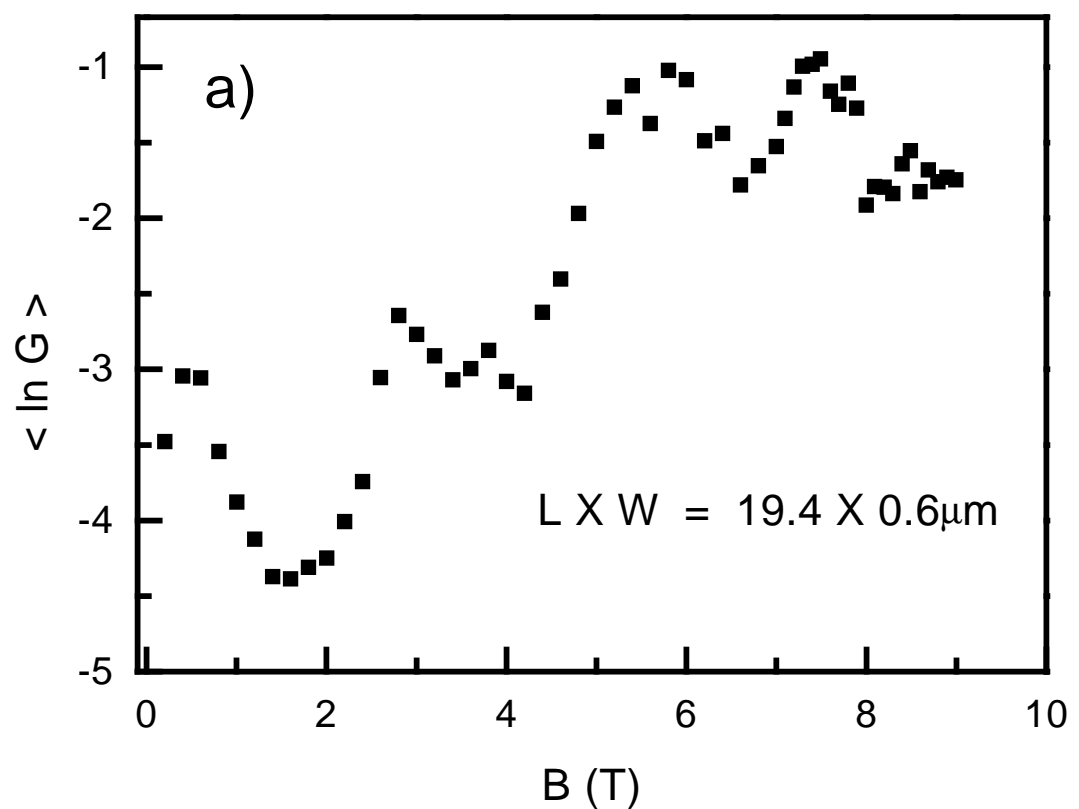


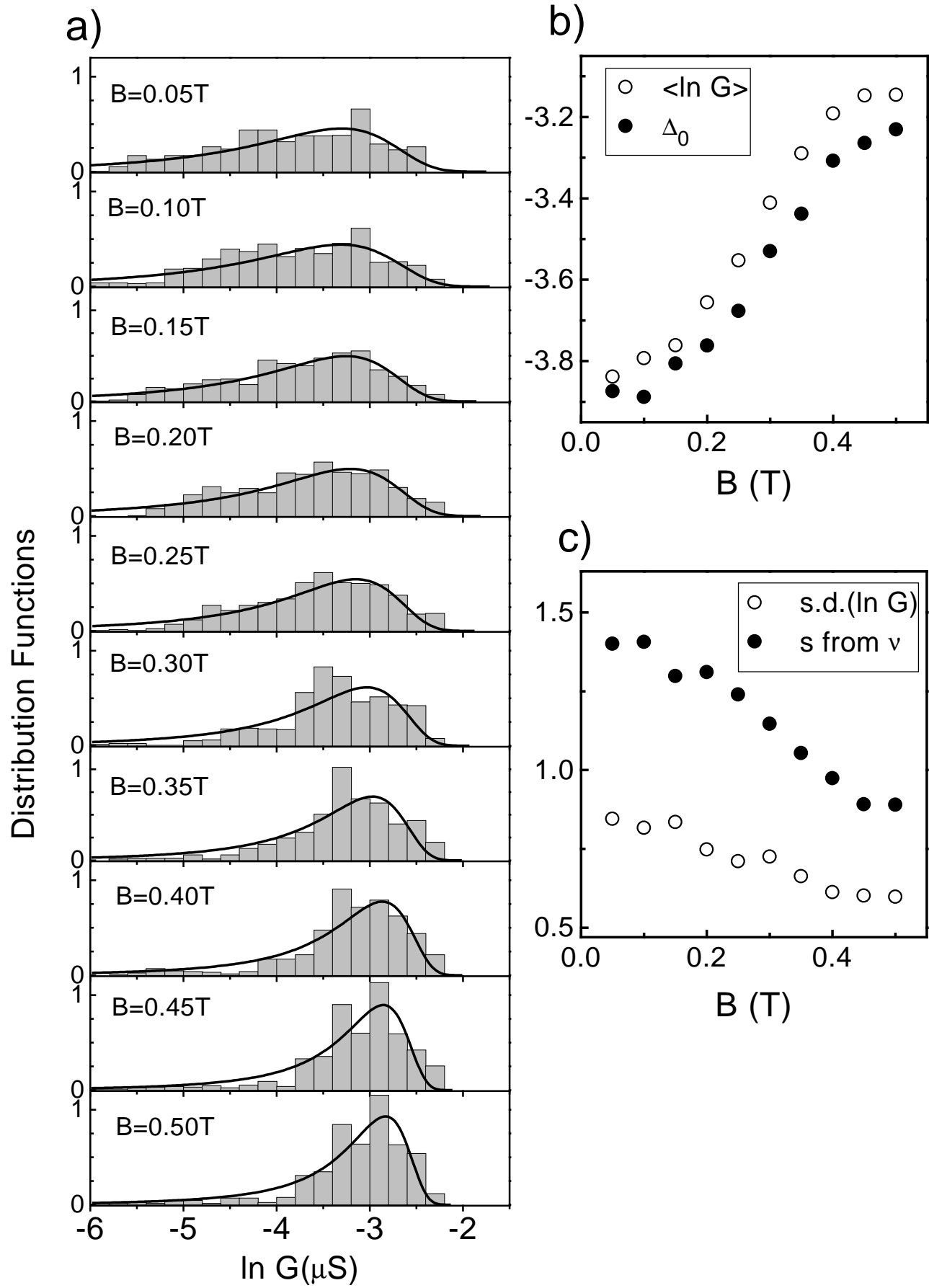












### Distribution Functions

